Synthesis and Characterization of Highly Luminescent CdS@ZnS Core−Shell Nanorods

Mee Rahn Kim, Young-Mee Kang, and Du-Jeon Jang*

School of Chemistry and Center for Space−Time Molecular Dynamics, Seoul National University, NS60, Seoul 151-742, Korea

Received: July 4, 2007; In Final Form: October 11, 2007

Highly luminescent CdS-core ZnS-shell nanorods stabilized by mercaptopropionic acid in water were synthesized wet-chemically and characterized by measuring photoluminescence spectra and kinetic profiles as well as absorption spectra, diffraction patterns, and electron microscope images. Photoluminescence from CdS nanorods 22 nm in diameter shifts to the blue by as much as 2.8 nm and increases as high as 1.8 times with the thickness of the passivating ZnS shell, whereas the luminescence lifetime of 1:1 CdS@ZnS core−shell nanorods is shorter by 1.6 times at 550 nm than that of bare CdS nanorods. Inorganic passivation by ZnS gives rise to the intensity increase and the lifetime decrease, while alloy formation with ZnS mainly brings about the blue shift.

Introduction

The spectroscopic, electronic, and chemical properties of nanostructured materials are of great interest in both basic and applied research.[1−4] Nanocomposites are even more attractive than individual single-component nanomaterials for a variety of solar photovoltaic devices, chemical/biological sensors, and optoelectronics such as light-emitting devices and optical switches,[5−9] so that various core−shell nanocomposites of semiconductor/semiconductor, carbon/metal, metal/semiconductor, and metal/metal have been fabricated.[2,10−12] Nanocomposites provide a wealth of opportunities for the controlled development of new materials and devices, as they exhibit improved physical and chemical properties over their single-component counterparts.

Nanosized semiconductor materials have drawn much research attention due to their potential applications for diverse electronic nanodevices.[7,8,13] As a large portion of atoms in nanocrystals is located at the surface, the codification of the surface has been recognized as one of the most advanced and intriguing methods to build tailored nanomaterials. It does not only alter the charge, the functionality, and the reactivity of the surface but also enhances the thermal, mechanical, and chemical stability of the material.[14,15] Thus, much effort has recently been invested in surface coating to create new classes of nanomaterials having novel optical, electrical, and magnetic properties.[5−7,16] Organically capped nanocrystals may still have a relatively large number of unpassivated surface sites due to the nature of passivating organic groups. For example, because II−VI semiconductors have anionic and cationic surface sites, it is very difficult for capping organic materials to passivate both types of surface sites simultaneously. In addition, the coverage of capping molecules is limited by steric effects because most of capped organic molecules are large and bulky in size.[17] Therefore, the surface control of nanocrystals has been a critical issue in enhancing photostability and luminescence efficiency.

Inorganically capped core−shell nanocomposites have revealed enhanced properties, as compared to those of respective original cores.[7,8,15] Thus, the fabrication of nanocomposites consisting of inorganic cores coated with various inorganic compositions has received considerable attention. The use of multicomponent semiconductor nanostructures provides an interesting opportunity for designing the electronic properties of materials.[18−20] Passivation of nanocomposite materials with semiconductors of higher band gaps is reported to improve luminescence quantum yields by decreasing nonradiative recombination.[18,19] Nanocomposite semiconductors coated with inorganic structures are much more robust than those coated with organic materials and have nonlinear optical properties.[19,21] Inorganic passivation eliminates both anionic and cationic dangling bonds at the surface and brings about new novel optical properties by reducing surface-related defect sites.[19,21−23] If the band gap of the core is enclosed by that of the shell, then the wave functions of electrons and holes may be confined within the core region, reducing the probability of nonradiative decay into surface states and trap sites.[22,23]

We have passivated CdS nanorods with ZnS, having a larger band gap of 3.66 eV than CdS with a gap of 2.53 eV, to enhance luminescence.[14] CdS and ZnS, important direct band gap materials of II−VI group semiconductors, have been extensively investigated.[24−26] CdS is typically sulfur-deficient with anion vacancies possessing a high electron affinity to make the material be *n*-type in nature. Photogenerated electrons and holes in CdS are well-separated to make charges highly localized, so that the luminescence lifetimes of CdS nanoparticles are long.[24] CdS is an excellent material with possible applications in optoelectronics such as nonlinear optics and light-emitting diodes, solar cells, and displays,[27,28] while ZnS is a well-known phosphor material having various advantageous properties such as efficient photoluminescence and electroluminescence. In this paper, we will show that the coating of CdS nanorods with ZnS enhances luminescence substantially while reducing the average lifetime of emission considerably.

Experimental Procedures

Materials. CdO(s), $Zn(NO_3)_2 \cdot 6H_2O$(s), $Na_2S \cdot 9H_2O$(s), elemental sulfur(s), mercaptopropionic acid(l), and ethylenediamine(l) were used as purchased from Sigma-Aldrich. Bare CdS

* Corresponding author. E-mail: djjang@snu.ac.kr.

10.1021/jp075218n CCC: $37.00
Published on Web 11/29/2007

nanorods were prepared by following the solvent-coordinating molecular template method of Li et al.[29] A total of 2.0 mmol of CdO(s), 2.0 mmol of elemental sulfur(s), and 40 mL of ethylenediamine(l) were put into a Teflon-lined stainless-steel autoclave of 50 mL, which was then sealed with an O-ring, placed in an oven at 180 °C for 30 h, and cooled to room temperature. The yellow precipitate of the product was separated by centrifugation, washed with deionized water and ethanol several times to remove residual impurities, and dried at 60 °C. For the preparation of mercaptopropionic acid-stabilized bare CdS nanorods in water, 0.173 g (1.2 mmol in CdS) of the previously prepared bare CdS nanorods was added into 300 mL of deionized water, which was then stirred violently for 30 min to ensure complete suspension. To the suspension was added 20 μL of mercaptopropionic acid(l) and refluxed with stirring at 70 °C for 2 h. For the synthesis of CdS-core ZnS-shell nanorods stabilized by mercaptopropionic acid in water, 30 mL of the previously prepared CdS colloidal solution was added with an appropriate amount of $Zn(NO_3)_2 \cdot 6H_2O$(s) and stirred for 1 h. The colloidal solution was then added with $Na_2S \cdot 9H_2O$-(s) having the same chemical amount as $Zn(NO_3)_2$, refluxed at 70 °C for 1 h, and cooled to room temperature. Finally, the aqueous colloidal solution of mercaptopropionic acid-stabilized bare ZnS nanoparticles was prepared by adding 0.12 mmol of $Na_2S \cdot 9H_2O$(s) and 20 μL of mercaptopropionic acid(l) into 30 mL of 4.0 mM $Zn(NO_3)_2$(aq) and by refluxing the mixture at 70 °C for 1 h.

Measurements. Selected-area electron diffraction (SAED) patterns and high-resolution transmission electron microscopy (HRTEM) images were measured by using a JEOL JEM-3000F microscope attached to a CCD camera as the detector. While transmission electron microscopy (TEM) images were obtained with a JEOL JEM-2000 microscope, high-resolution X-ray diffraction (HRXRD) patterns were recorded with a Bruker D8 DISCOVER diffractometer using Cu Kα radiation. Absorption spectra were measured by using a Scinco S-3100 UV−vis spectrometer, and photoluminescence spectra were detected by using a CCD from Princeton Instruments ICCD576G with excitation of 355 nm pulses from a Q-switched Nd:YAG laser from Quantel Brilliant. Photoluminescence kinetic profiles were measured with a 10 ps streak camera from Hamamatsu C2830 attached with a CCD detector from Princeton Instruments RTE128H after exciting colloidal samples at 355 nm with a 25 ps actively/passively mode-locked Nd:YAG laser of Quantel YG701. The decay constants of photoluminescence were extracted by fitting measured kinetic profiles to computer-simulated exponential curves convoluted with instrument response functions.

Results and Discussion

Figure 1a shows a typical TEM image of bare CdS nanorods having an average diameter of 22 ± 3 nm, which were prepared by using a solvent-coordinating molecular template of ethylenediamine. Although bare CdS nanorods were aggregated during evaporation for the TEM measurement, their crystalline structures can be discerned easily in Figure 1b as well. Furthermore, the clear lattice fringes and the smooth surface of a bare CdS nanorod indicate that the structure is single crystalline. The SAED spot pattern of Figure 1c suggests that bare CdS nanorods have the crystalline structure of wurtzite CdS. The measured interplanar distance of 0.34 nm, indicated by two white lines in Figure 1b, corresponds to the spacing of the (002) planes of the wurtzite CdS.

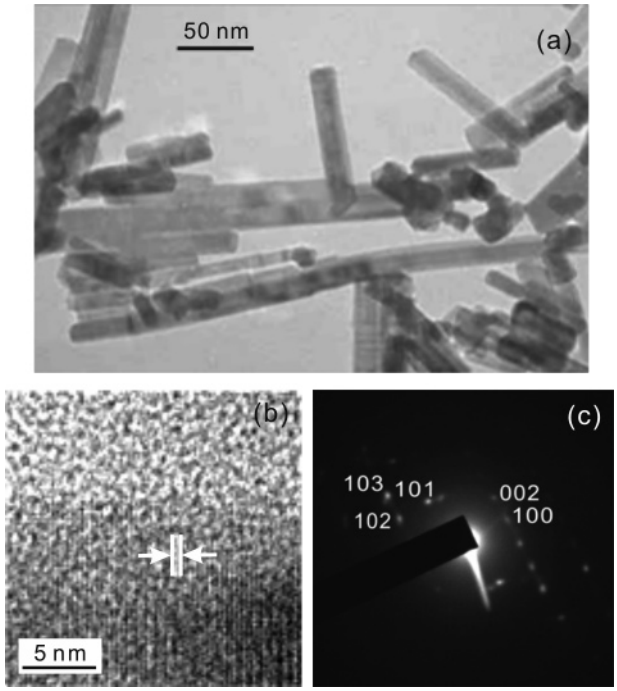

Figure 1. TEM image of typically prepared bare CdS nanorods (a) and HRTEM image (b) and SAED pattern (c) of a bare CdS nanorod. The distance between the two white lines in panel b is 0.34 nm.

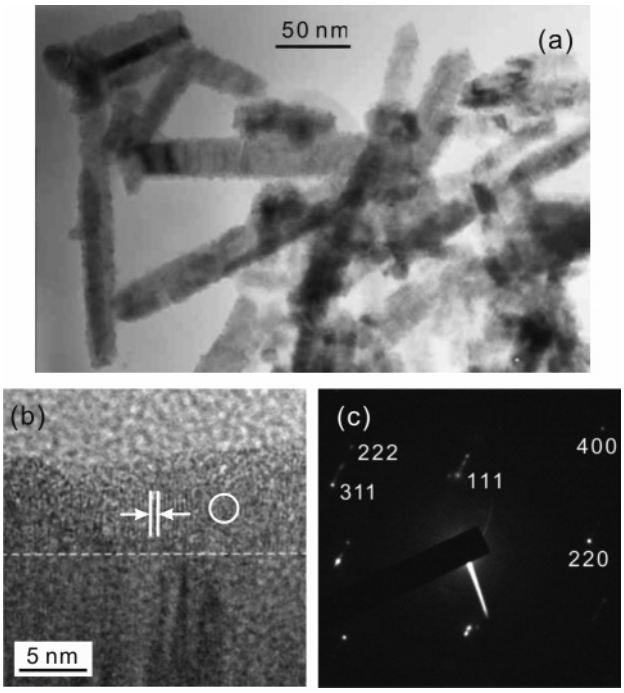

Figure 2. TEM image of typically prepared 1:1 CdS@ZnS core−shell nanorods (a), HRTEM image of a 1:1 CdS@ZnS core−shell nanorod (b), and SAED pattern of the shell area indicated by the circle in panel b (c). While the dashed white line in panel b indicates the approximate interface of the core and the shell, the distance between the two solid white lines in panel b is 0.31 nm.

The TEM image of Figure 2a indicates that our fabricated 1:1 CdS@ZnS core−shell nanorods have rougher surfaces and slightly larger diameters than the bare CdS nanorods in Figure 1a. However, one can see that the lengths of nanorods remain almost invariant with passivation. The HRTEM image of a CdS@ZnS nanorod in Figure 2b shows a distinguishable interface, highlighted by a dashed line, between the CdS core and the ZnS shell due to variations in electron density and

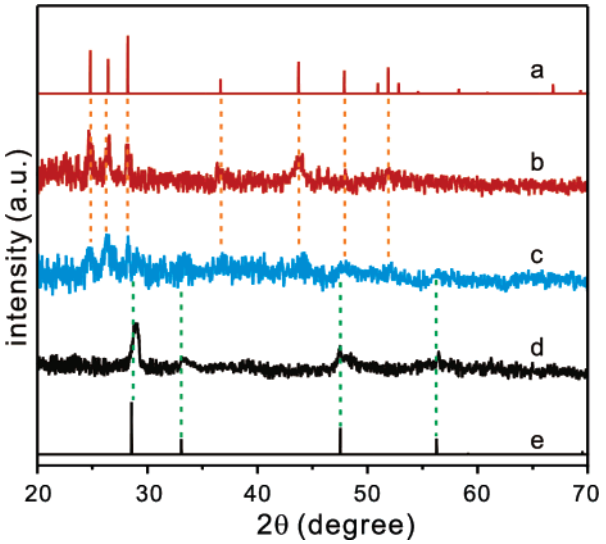

Figure 3. HRXRD patterns of reference wurtzite CdS (a), bare CdS nanorods (b), 1:1 CdS@ZnS core−shell nanorods (c), ZnS nanoparticles (d), and reference zinc-blende ZnS (e).

crystalline structure. CdS nanorods in CdS@ZnS core−shell nanorods are well-overcoated by ZnS with an approximate thickness of 3 nm. The SAED spot pattern of Figure 2c indicates that the ZnS shell of a CdS@ZnS nanorod has the crystalline structure of zinc-blende ZnS. The measured lattice−fringe distance of 0.31 nm, indicated by two white lines in Figure 2b, agrees well with the spacing of the (111) planes of the zinc-blende ZnS. Because the lattice spacing of the shell ZnS is very similar to that of the core CdS, passivation can be carried out uniformly with a minor atomic level reconstruction of the surface.[30]

HRXRD patterns in Figure 3 show that a 1:1 CdS@ZnS core−shell nanorod has composite diffraction peaks arising from both wurtzite CdS and zinc-blende ZnS. Although CdS@ZnS nanoparticles with thick shells were reported to show diffraction peaks only from the shell ZnS,[30] our 1:1 CdS@ZnS nanorods with l_{shell}/d_{core} of 0.2, where l_{shell} and d_{core} designate the shell thickness and the core diameter, respectively, show diffraction peaks from the cores as well as those from the shells. The four primary strong diffraction peaks at 2θ of 24.83, 26.45, 28.22, and 44.19 and the three secondary weak diffraction peaks at 2θ of 28.56, 33.12, and 56.49 also indicate that the core and the shell have the crystalline structures of wurtzite CdS and zinc-blende ZnS, respectively, as already described in Figures 1 and 2.

The extinction spectra of Figure 4 show that the absorption band edges of CdS@ZnS core−shell nanorods are at 495 ± 2 nm (2.50 eV) and that there is a slight blue shift with shell thickness in the absorption edge due to the influence of the shell ZnS, although it is difficult to observe the absorption edge because of prevailing scattering. The drastic increase of extinction with ZnS addition is attributed to scattering increased exponentially with the size increment of CdS@ZnS nanorods. The band edges of CdS@ZnS heterostructures (the type I hybrid semiconductors) are dominated by the core, whose both conduction and valence bands are included in those of the shell. The electrons and the holes of CdS@ZnS nanorods experience potential confinement that tends to localize both carriers in the core nanocrystals. Thus, the passivation of CdS nanorods with ZnS improves the emission quantum yields of the core nanocrystals to bring in efficient photoluminescence.[18,22,31]

Figure 5 shows that the emission maximum of CdS@ZnS

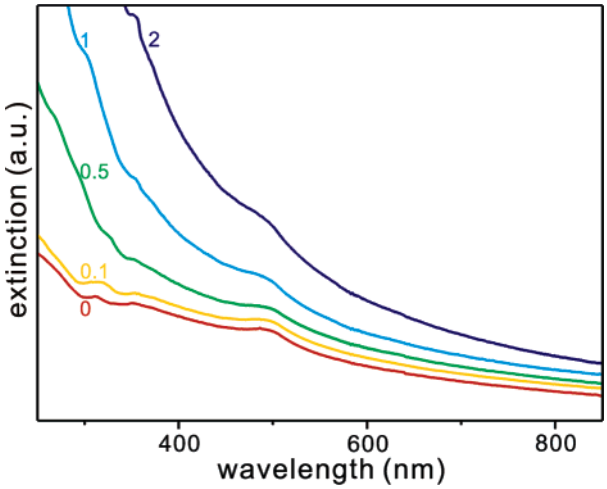

Figure 4. Extinction spectra of mercaptopropionic acid-stabilized CdS@ZnS nanocomposites dispersed in water. Numbers near spectra indicate molar ratios of ZnS/CdS, while the molar concentrations of CdS are fixed to be 4.0 mM in all the spectra.

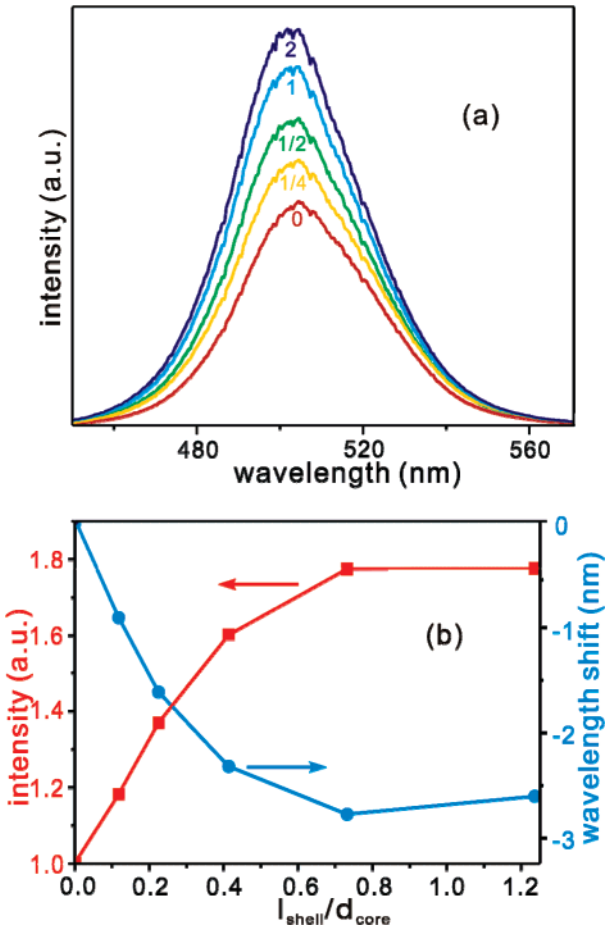

Figure 5. Photoluminescence spectra of mercaptopropionic acid-stabilized CdS@ZnS nanocomposites in water at indicated various values of [ZnS]/[CdS] with 4.0 mM [CdS] after excitation at 355 nm (a) and the variations of the peak intensity (squares) and the wavelength shift (circles) of the photoluminescence with l_{shell}/d_{core} (b).

nanorods in water shifts to the blue with the thickness of the shell, while that of bare CdS nanorods with excitation at 355 nm is at 506.9 nm. As described in Figure 4, this suggests that although the band edge emission of CdS@ZnS is dominated spectrally by the core CdS, it shifts to the blue with ZnS passivation owing to the partial formation of a $Cd_{1-x}Zn_xS$ alloy between the core and the shell.[32] It has been reported[30,33] that

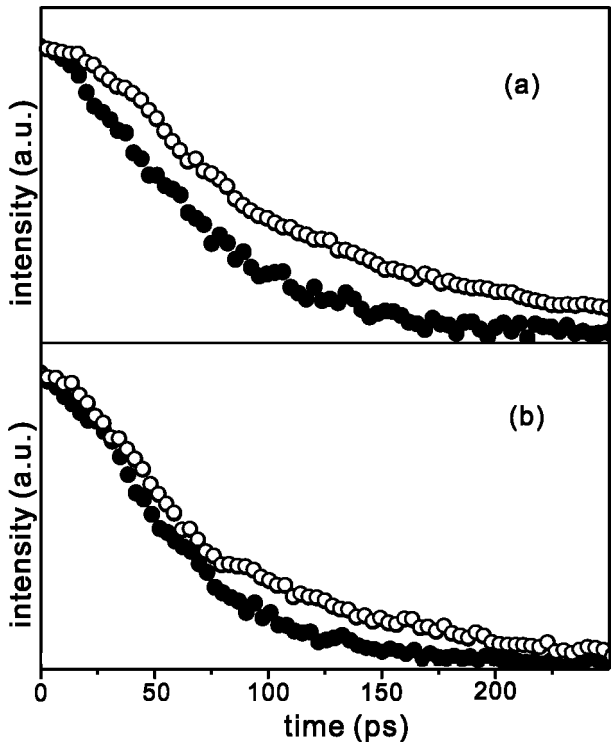

Figure 6. Luminescence decay kinetic profiles of bare CdS nanorods (a) and 1:1 CdS@ZnS nanorods (b) stabilized by mercaptopropionic acid in water, monitored at 480 nm (closed) and 550 nm (open) after excitation at 355 nm. The molar concentrations of CdS in both samples are 4.0 mM.

photoluminescence from both the particle films and the coaxial nanowires of CdS@ZnS shift to the blue with the extent of ZnS coating. The almost symmetrically simultaneous blue shifts of the blue and the red half-maxima of the emission suggest that the decrease of the surface state emission with the shell thickness contributes inconsiderably to the shift, although it enhances photoluminescence extensively. As already shown in Figure 2, the partial formation of a $Cd_{1-x}Zn_xS$ alloy also implies that the passivation of CdS with ZnS has been carried out smoothly because of the similar lattice parameters of CdS and ZnS to each other. Figure 5 indicates that the photoluminescence of CdS@ZnS nanorods increases as high as 1.8 times with the shell thickness of ZnS. This is attributed to the blocked quenching of photoexcited electrons in the conduction band into the surface-trap states of a CdS nanorod by the ZnS shell. It is generally known that the most vacancies of CdS nanoparticles are on the surfaces and lead to the nonradiative recombination of electrons and holes.[29] Photoluminescence from band edge states is reduced exceedingly with the high surface-to-volume ratio of a nanorod because the surface-trap states are expanded with the ratio.[34,35] Additionally, the delocalization of carriers increases nonradiative recombination due to the decreased overlaps between the wave functions of electrons and holes.[14,32,35] ZnS overcoating suppresses the quenching of photoexcited electrons into deep- or surface-trap sites by passivating vacancies and trap sites on the surfaces of CdS nanocrystallites, enhancing photoluminescence greatly.[32,35]

Figure 6 reveals that the photoluminescence kinetic profiles of both bare CdS and core−shell CdS@ZnS nanorods decay faster at 480 nm than at 550 nm. This suggests that the emission at 480 nm arises mainly from electrons in the conduction band of CdS, while that at 550 nm has an additional contribution from the trap sites of CdS.[36] The kinetic differences between bare and core−shell nanorods are not obvious at first glance of Figure 6. However, the extracted kinetic constants of Table 1 indicate that the emission of core−shell nanorods at 550 nm decays faster by 1.6 times than that of bare nanorods, whereas the decay kinetic profiles of both samples have similar time constants at 480 nm. Because emission decays faster at 480 nm than at 550 nm, we have fitted observed kinetic profiles into double-exponential decay curves of ~35 and 120 ps. The fast and slow time constants have been attributed to the emission decay time of electrons in the conduction band of CdS and that at the trap sites of CdS, respectively. As suggested previously, the dominant amplitude percentage of the fast component indicates indeed that photoluminescence at 480 nm results essentially from the band gap emission of the core CdS. On the other hand, the amplitude percentage of the slow component at 550 nm has been decreased substantially with ZnS passivation. This designates that the quenching of the ensnaring of conduction band electrons into the trap sites by ZnS passivation, thus reducing the nonradiative recombination of electrons and holes at trap sites, results in a large increase of CdS photoluminescence with the thickness of the ZnS shell shown in Figure 5. Thus, Figures 5 and 6 indicate that the photoluminescence of CdS nanorods increases enormously, whereas its lifetime decreases greatly with ZnS coating. This intimates that passivation with ZnS enhances the optical properties of CdS nanorods substantially.

TABLE 1: Decay Kinetic Constants Deconvoluted from the Profiles of Figure 6

Figure	[ZnS]/[CdS]	λ_{mon}[a] (nm)	mean lifetime (ps)	lifetime (ps)
6a	0	480	36	30 (93%) + 120 (7%)[b]
		550	80	37 (48%) + 120 (52%)
6b	1	480	37	35 (98%) + 120 (2%)
		550	49	37 (85%) + 120 (15%)

[a] Monitored wavelength of photoluminescence. [b] Initial intensity percentage of each component.

Conclusion

CdS-core ZnS-shell nanorods, prepared wet-chemically and stabilized by mercaptopropionic acid in water, were found to have improved optical properties as compared to bare CdS nanorods. Photoluminescence from CdS nanorods 22 ± 3 nm in diameter increased with the thickness of the passivating ZnS shell as high as 1.8 times, although the luminescence lifetime of 1:1 CdS@ZnS core−shell nanorods is shorter by 1.6 times at 550 nm than that of bare CdS nanorods. On the other hand, the emission maximum of CdS@ZnS nanorods shifts to the blue as large as 2.8 nm with the thickness of the shell. The increase of photoluminescence and the decrease of emission lifetime are attributed to the quenching of electron ensnaring into trap sites by passivation, while the blue shift of photoluminescence is ascribed to the partial formation of a $Cd_{1-x}Zn_xS$ alloy between the core and the shell.

Acknowledgment. This work was financially supported by the Korea Science and Engineering Foundation Grant M10703000871-07M0300-87110 funded by the Korea Ministry of Science and Technology. M.R.K. also acknowledges a scholarship from the BK21 Program.

References and Notes

(1) Chung, J. H.; Ah, C. S.; Jang, D.-J. *J. Phys. Chem. B* **2001**, *105*, 4128.
(2) Ah, C. S.; Kim, S. J.; Jang, D.-J. *J. Phys. Chem. B* **2006**, *110*, 5486.
(3) Kim, S. J.; Ah, C. S.; Jang, D.-J. *Adv. Mater.* **2007**, *19*, 1064.

(4) Kim, M. R.; Kim, J. Y.; Jang, D.-J. *Eur. Phys. J. D* **2007**, *43*, 279.
(5) Santra, S.; Yang, H.; Holloway, P. H.; Stanley, J. T.; Mericle, R. A. *J. Am. Chem. Soc*. **2005**, *127*, 1656.
(6) Kim, J. Y.; Osterloh, F. E. *J. Am. Chem. Soc.* **2005**, *127*, 10152.
(7) Ipe, B. I.; Niemeyer, C. M. *Angew. Chem., Int. Ed.* **2006**, *45*, 504.
(8) Yang, Y.; Chen, O.; Angerhofer, A.; Cao, Y. C. *J. Am. Chem. Soc*. **2006**, *128*, 12428.
(9) Ouyang, L.; Maher, K. N.; Yu, C. L.; McCarty, J.; Park, H. *J. Am. Chem. Soc.* **2007**, *129*, 133.
(10) Kim, M. R.; Ahn, S. J.; Jang, D.-J. *J. Nanosci. Nanotechnol*. **2006**, *6*, 180.
(11) Kim, Y.-T.; Ohshima, K.; Higashimine, K.; Uruga, T.; Takata, M.; Suematsu, H.; Mitani, T. *Angew. Chem., Int. Ed.* **2006**, *45*, 407.
(12) Subramanian, V.; Wolf, E. E.; Kamat, P. *J. Am. Chem. Soc*. **2004**, *126*, 4943.
(13) Yu, D.; Wu, J.; Gu, Q.; Park, H. *J. Am. Chem. Soc.* **2006**, *128*, 8148.
(14) Trindade, T.; O'Brien, P.; Pickett, N. L. *Chem. Mater*. **2001**, *13*, 3843.
(15) Pan, A.; Wang, S.; Liu, R.; Li, C.; Zou, B. *Small* **2005**, *1*, 1058.
(16) Wang, D.; He, J.; Rosenzweig, N.; Rosenzweig, Z. *Nano Lett.* **2004**, *4*, 409.
(17) Ni, T.; Nagesha, D. K.; Robles, J.; Materer, N. F.; Müssig, S.; Kotov, N. A. *J. Am. Chem. Soc.* **2002**, *124*, 3980.
(18) Balet, L. P.; Ivanov, S. A.; Piryatinski, A.; Achermann, M.; Klimov, V. I. *Nano Lett.* **2004**, *4*, 1485.
(19) Yang, H.; Holloway, P. H. *Adv. Funct. Mater*. **2004**, *14*, 152.
(20) Kim, S.; Fisher, B.; Eisler, H.-J.; Bawendi, M. *J. Am. Chem. Soc*. **2003**, *125*, 11466.
(21) Peng, X.; Schlamp, M. C.; Kadavanich, A. V.; Alivisatos, A. P. *J. Am. Chem. Soc.* **1997**, *119*, 7019.
(22) Mokari, T.; Banin, U. *Chem. Mater*. **2003**, *15*, 3955.
(23) Dabbousi, B. O.; Rodriguez-Viejo, J.; Mikulec, F. V.; Heine, J. R.; Mattoussi, H.; Ober, R.; Jensen, K. F.; Bawendi, M. G. *J. Phys. Chem. B* **1997**, *101*, 9463.
(24) Zhang, J. Z. *J. Phys. Chem. B* **2000**, *104*, 7239.
(25) Agarwal, R.; Barrelet, C. J.; Lieber, C. M. *Nano Lett.* **2005**, *5*, 917.
(26) Logunov, S.; Green, T.; Marguet, S.; El-Sayed, M. A. *J. Phys. Chem. A* **1998**, *102*, 5652.
(27) Yao, W.-T.; Yu, S.-H.; Liu, S.-J.; Chen, J.-P.; Liu, X.-M.; Li, F.-Q. *J. Phys. Chem. B* **2006**, *110*, 11704.
(28) Pan, A.; Liu, R.; Yang, Q.; Zhu, Y.; Yang, G.; Zou, B.; Chen, K. *J. Phys. Chem. B* **2005**, *109*, 24268.
(29) Li, Y.; Liao, H.; Ding, Y.; Fan, Y.; Zhang, Y.; Qian, Y. *Inorg. Chem.* **1999**, *38*, 1382.
(30) Hsu, Y.-J.; Lu, S.-Y.; Lin, Y.-F. *Adv. Funct. Mater*. **2005**, *15*, 1350.
(31) Hsu, Y.-J.; Lu, S.-Y. *Langmuir* **2004**, *20*, 194.
(32) Xie, R.; Kolb, U.; Li, J.; Basché, T.; Mews, A. *J. Am. Chem. Soc.* **2005**, *127*, 7480.
(33) Pan, D.; Wang, Q.; Jiang, S.; Ji, X.; An, L. *Adv. Mater*. **2005**, *17*, 176.
(34) El-Sayed, M. A. *Acc. Chem. Res.* **2004**, *37*, 326.
(35) Manna, L.; Scher, E. C.; Li, L.-S.; Alivisatos, A. P. *J. Am. Chem. Soc.* **2002**, *124*, 7136.
(36) Chae, W.-S.; Shin, H.-W.; Lee, E.-S.; Shin, E.-J.; Jung, J.-S.; Kim, Y.-R. *J. Phys. Chem. B* **2005**, *109*, 6204.